Determination of Interatomic Potentials from the Far Wings of Spectral Lines Perturbed by Neutral Atoms

J. Losen and W. Behmenburg

Physikalisches Institut der Universität Düsseldorf

(Z. Naturforsch. **28 a**, 1620—1634 [1973]; received 21 March 1973)

An indirect method for the determination of interatomic potentials from measurements of the far wings of atomic absorption lines perturbed by neutral atoms is described. In this method the potential parameters are derived by optimum adjustment of line shapes calculated on the basis of the PHQSB-theory (binary approximation of the quasistatic theory of line broadening), assuming Lennard-Jones interaction, to measured profiles of an atomic absorption line perturbed by neutral atoms. The method is applied to measurements of the Hg-absorption line λ 2537 Å, perturbed by Ar and Hg at an Ar number density of 1.26×10^{19} cm^{-3} and Hg number densities between 7.4×10^{16} and 3.36×10^{18} cm^{-3}, corresponding to temperatures between 427 and 563.5 °K. The reliability of the resulting L.-J.-parameters is discussed by considering the validity criteria of the PHQSB-theory and by comparison with potential curves obtained from other spectroscopic data.

I. Introduction

Many macroscopic properties of matter are determined by intermolecular forces. Their exact quantummechanical calculation is very difficult, even in simple cases. Therefore experimental methods for their determination are of particular importance.

Until recently, information on interatomic forces have been derived mainly from molecular beam experiments. Such information, however, is largely restricted to interaction between atoms in the electronic ground state. On the other hand, information on excited state interaction may be derived from optical methods, one of which, the method of collision broadening of spectral lines by neutral atoms, is mainly discussed at present.

So far measurements of collision broadening have been mainly restricted to total crossections, the crossections for halfwidth and shift of the line [1–4]. Much more information on interatomic forces may be derived, however, from the differential crossection, namely the spectral intensity distribution of the line, especially its far wings. Measurements of the far wings offer themselves particularly well for two reasons. First, because of the slow intensity change in the far wings, the requirements for resolving power of the monochromator need not be too extreme. Secondly, at sufficiently low particle number densities the far wing spectra are comparatively simply related to the potential functions through the binary approximation of the quasistatic theory of line broadening (PHQSB-theory) [5]. In certain cases, depending on the behaviour of the potential functions, the PHQSB-theory is, in the far wings, a good approximation to the general phase shift theory of collision broadening.

On the basis of the PHQSB-theory, the true difference potential, which may be very complicated, may be obtained directly from far wing measurements, without relying on any particular model function. An appropriate method of evaluation (direct method) has been reported in a preceeding paper [6]. In the present investigation the experimental results are interpreted in terms of potential functions of the Lennard-Jones-(L.-J.-)type; the potential parameters were determined by optimum adjustment of the theoretical to the experimental profiles. This indirect method has several advantages. First, due to the simplicity of the PHQSB-theory and of the L.-J.-potential function, the influence of the various factors on the wing profiles (like the shape of the difference potential and the radial distribution function) may easily be investigated by calculation. Furthermore, by comparison with the results of the direct method, the reliability of this method may be tested and the degree of approximation of the L.-J.-potential to the true potential functions investigated. Finally, the use of a model function facilitates the derivation of explicit analytical expressions for the validity ranges of the PHQSE-theory, on which both methods for the determination of the potential functions are based.

The indirect method is applied to measurements of the far wings of the Hg absorption line λ 2537 Å

Reprint requests to Dr. W. Behmenburg, Physikalisches Institut der Universität Düsseldorf, *D-4000 Düsseldorf*, Moorenstraße 5, Institutsgruppe 1, Bau A.

perturbed by Ar and Hg. The measurements are performed at number densities $n_{Ar} = 1.26 \times 10^{19}\,cm^{-3}$ and $7.4 \times 10^{16} \leqq n_{Hg} \leqq 3.36 \times 10^{18}\,cm^{-3}$ with temperatures in the range $427 \leqq T \leqq 563.5\,°K$. Under these conditions the assumptions of the PHQSE-theory are well fufilled for the systems under consideration, as will be shown in Chapter VI, 2.

II. Theory

1. Basic Assumptions and General Intensity Formula

In the PHQSB-theory the following assumptions are made:

a) The active atom is surrounded by perturbers, which are at rest relative to the active atom. This is equivalent with assuming, that the contributions of the collisions to the spectrum are negligable.

b) Only the effect of the nearest perturber is taken into account. This means, that the number density of the perturber is assumed to be sufficiently small.

c) The oscillator strength of the line under investigation is assumed to be independent of the internuclear distance in the energy range considered.

Under these assumptions the radiation intensity $I(\Delta\omega)\,d(\Delta\omega)$ absorbed or emitted in the frequency interval between $\Delta\omega$ and $\Delta\omega + d(\Delta\omega)$ is then proportional to the probability of finding the nearest perturber at distances r_k, where it just produces the frequency perturbation $\Delta\omega$

$$I(\Delta\omega)\,d(\Delta\omega) = \sum_k W(r_k)\,dr_k\,^* . \tag{1}$$

$r(\Delta\omega)$ is generally a multivalued function determined by the difference of the potentials $V^{i,f}(r)$ for the initial and final states of the system:

$$\hbar\,\Delta\omega = V(r) \equiv V^f(r) - V^i(r) . \tag{2}$$

If the difference potential $V(r)$ is of the L.-J.-type, $r(\Delta\omega)$ is in general double valued. Thus we have in this case

$$I(\Delta\omega)\,d(\Delta\omega = W(r_1)\,dr_1 + W(r_2)\,dr_2 . \tag{3}$$

The distribution function $W(r)$ is, in case of thermodynamic equilibrium, given by **

$$W(r) = 4\pi r^2 n \exp\{-V^i(r)/kT\} \cdot g(r) \tag{4}$$

where n is the particle number density and $g(r)$ is the relative number of unbound pairs [7]:

$$g(r) = (2/\sqrt{\pi})\{\sqrt{x_0}\exp\{-x_0\} + (\sqrt{\pi}/2)(1 - \mathrm{erf}(\sqrt{x_0}))\} \tag{5}$$

with

$$x_0 = -V^i(p)/kT$$

and

$$\mathrm{erf}(\sqrt{x_0}) = (2/\sqrt{\pi})\int_0^{\sqrt{x_0}} \exp\{-z^2\}\,dz .$$

2. Influence of the Potentials $V(r)$ and $V^i(r)$ on the Wing Shape

Assume for a moment, that in the differential Eq. (3) the first term on the right hand side is negligably small compared to the second term (we shall see later in which cases this assumption is fulfilled). Then (3) may be rewritten, using (2)

$$I(\Delta\omega) \sim W(r)\,\frac{1}{dV(r)/dr} . \tag{6}$$

The spectral intensity distribution in the wings is thus determined by two factors: the difference potential $V(r)$, more precisely by its change with internuclear distance r, and, through the distribution function, by the initial state potential $V^i(r)$.

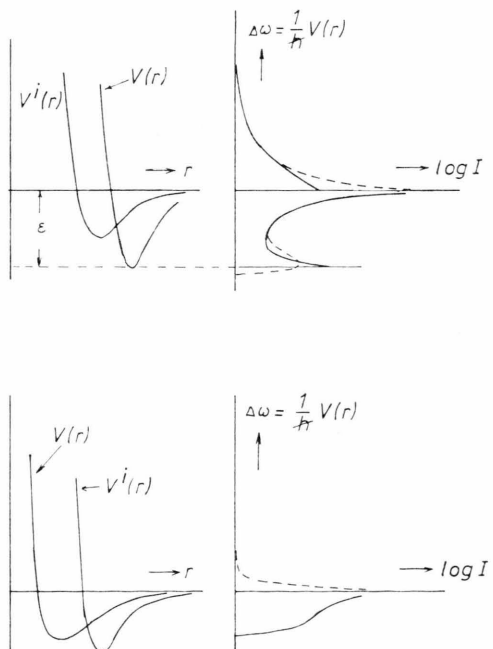

Fig. 1. Influence of the relative positions of the potentials $V^i(r)$ and $V(r)$ on the wing shape.

* Assuming $\int I(\Delta\omega)\,d(\Delta\omega) = 1$.

** Apart from a normalization factor, which is very close to unity at sufficiently small particle number densities.

In particular, in the range $V^{i}(r)>0$, where $|\mathrm{d}V^{i}(r)/\mathrm{d}r|$ is large, $I(\Delta\omega)$ will be mainly determined by $V^{i}(r)$. In the range $V^{i}(r)<0$, its influence on $I(\Delta\omega)$ will be noticable only if $|V^{i}(r)/kT|$ is ≈ 1 or $\gg 1$.

A more detailed consideration shows, that the shape of the wings is determined by the relative position of $V(r)$ and $V^{i}(r)$. Two cases have to be distinguished (Fig. 1) depending on whether σ^{i}, the zero of $V^{i}(r)$ is smaller or larger than σ, the zero of $V(r)$.

1) $\sigma^{i}<\sigma$

Due to the extremum in $V(r)$ a secondary intensity maximum (satellite) is expected at a frequency distance $|\Delta\omega|=\varepsilon/\hbar$ from the unperturbed line. Depending on whether the extremum is a minimum or a maximum, the satellite will appear on the red or blue side of the line. This type of satellite, which is not of molecular origin, has its analogon in the rainbow effect in atomic beam scattering, namely the maximum in the differential scattering crossection as a function of the scattering angle. A great number of satellites have been actually observed [8, 9]. But it is not sure whether they are all due to extrema in the difference potential. For the red satellite of the $P_{1/2}$-component of the potassium resonance line perturbed by Krypton McCartan and Hindmarsh [10] have given an interpretation in terms of the L.-J.-potential consistently describing the total line profile.

2) $\sigma^{i}>\sigma$

No satellite is to be expected in this case, but a steep monotonic intensity decrease instead. The reason is, that the extremum of $V(r)$ does not become effective, sinve already at $r>\sigma$ $V^{i}(r)>0$ rapidly increases, thus causing a rapid decrease of the distribution function. This case is realized for example at the $^{1}\Sigma_{0}\rightarrow{}^{3}\Pi_{0}$-transition of the systems Hg 2537/ noble gas, discussed in this paper.

3. The Calculation of the Wings Assuming L.-J.-Interaction, Neglecting Molecular Formation

Distinguishing between the difference potential $V(r)$ and the initial state potential $V^{i}(r)$, we have in case of L.-J.-6-12-interaction

$$V(r)_{\mathrm{LJ}}=-C_{6}/r^{6}+C_{12}/r^{12} \quad \text{and} \tag{7}$$

$$V^{i}(r)_{\mathrm{LJ}}=-C_{6}^{i}/r^{6}+C_{12}^{i}/r^{12} \tag{8}$$

(7) and (8) may be written in the alternative form

$$V(r)_{\mathrm{LJ}}=4\,\varepsilon[-(\sigma/r)^{6}\pm(\sigma/r)^{12}] \tag{7'}$$

(upper sign for $C_{12}/C_{6}>0$, lower sign for $C_{12}/C_{6}<0$) and

$$V^{i}(r)_{\mathrm{LJ}}=-4\,\varepsilon^{i}[-(\sigma^{i}/r)^{6}+(\sigma^{i}/r)^{12}] \tag{8'}$$

where the ε's and σ's refer to the depths and zeros of the potential wells, respectively. These quantities are related to the quantities C_{6}, C_{6}^{i} and C_{12}, C_{12}^{i} by

$$\sigma=|C_{12}/C_{6}|^{1/6};\quad \varepsilon=\tfrac{1}{4}\,C_{6}^{2}/C_{12}\,; \tag{9}$$

$$\sigma^{i}=(C_{12}^{i}/C_{6}^{i})^{1/6};\quad \varepsilon^{i}=\tfrac{1}{4}\,C_{6}^{i2}/C_{12}^{i}\,. \tag{9'}$$

Neglecting the formation of molecules, the function $g(r)$ in (4) becomes unity and the general expression for the intensity becomes

$$I(\Delta\omega)\,\mathrm{d}(\Delta\omega)=\sum_{k=1}^{2}W(r_{k})\,\mathrm{d}r_{k}$$
$$=4\pi n\sum_{k=1}^{2}r_{k}^{2}\,\mathrm{d}r_{k}\exp\{-V^{i}(r_{k})/kT\}\,. \tag{10}$$

For the evaluation of the intensity formula (10) it is sufficient to consider two cases:

1) $C_{6}>0$, $C_{12}>0$

In this case the sum in (10) reduces to a single term in the range $r<\sigma$. Introducing dimensionless quantities

$$\begin{aligned} &x_{k}=r_{k}/\sigma;\quad k=1,2;\\ &y=\hbar\,\Delta\omega/\varepsilon;\\ &L=\sigma^{i}/\sigma;\quad C=\varepsilon^{i}/kT \end{aligned} \tag{11}$$

and the abbreviations

$$\begin{aligned} &f=(1+y/2)/(1+y)^{1/2};\quad f_{1}=1+(1+y)^{1/2};\\ &f_{2}=1-(1+y)^{1/2}; \end{aligned} \tag{12}$$

$$V_{k}(L,y)\equiv V^{i}(r_{k})/\varepsilon^{i}=-2\,L^{6}f_{k}(y)+L^{12}f_{k}^{2}(y)$$

one obtains for $y<0$ (red wing)

$$\begin{aligned} I(y,L,C)=&\frac{\sqrt{2}}{3}\,h\,n\,\frac{\sigma^{3}}{\varepsilon}\\ &\cdot y^{-2}\{|1-f(y)|\,|f_{1}(y)|^{1/2}\exp[-C\,V_{1}(L,y)]\\ &+|1+f(y)|\,|f_{2}(y)|^{1/2}\exp[-C\,V_{2}(L,y)]\} \end{aligned} \tag{13}$$

and for $y>0$ (blue wing)

$$\begin{aligned} I(y,L,C)=&\frac{\sqrt{2}}{3}\,h\,n\,\frac{\sigma^{3}}{\varepsilon}\\ &\cdot y^{-2}\{|1-f(y)|\,|f_{1}(y)|^{1/2}\exp[-C\,V_{1}(L,y)]\}\,. \end{aligned} \tag{14}$$

Figures 2 – 5 demonstrate the dependence of the wing shape on the relative position of $V(r)$ and

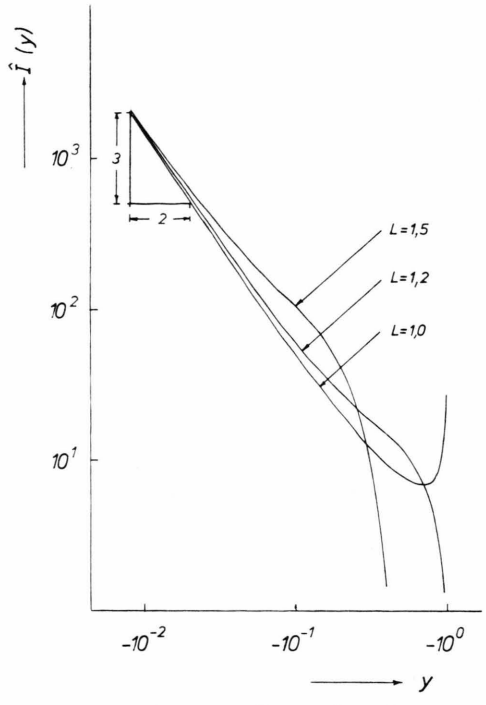

Fig. 2. PHQSB-theory, $C_6>0$, $C_{12}>0$; $C=1.0$; L-dependence of the red wing.

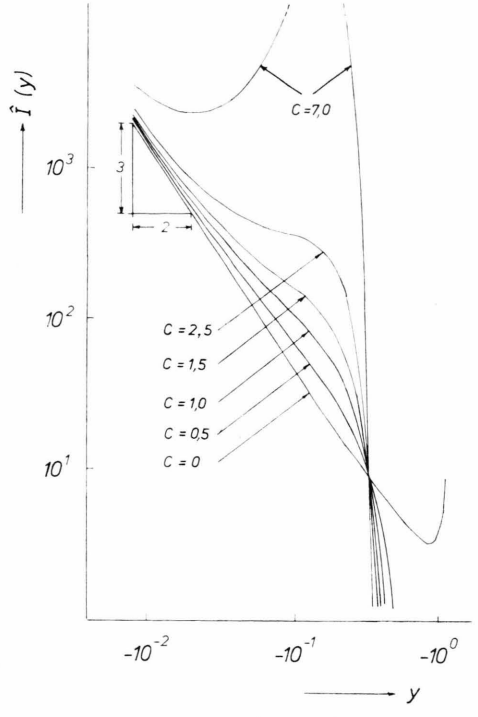

Fig. 4. PHQSB-theory, $C_6>0$, $C_{12}>0$; $L=1.5$; C-dependence of the red wing.

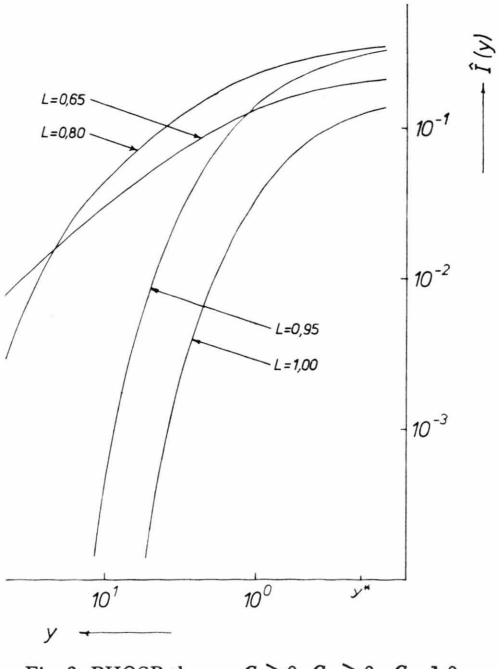

Fig. 3. PHQSB-theory, $C_6>0$, $C_{12}>0$; $C=1.0$; L-dependence of the blue wing.

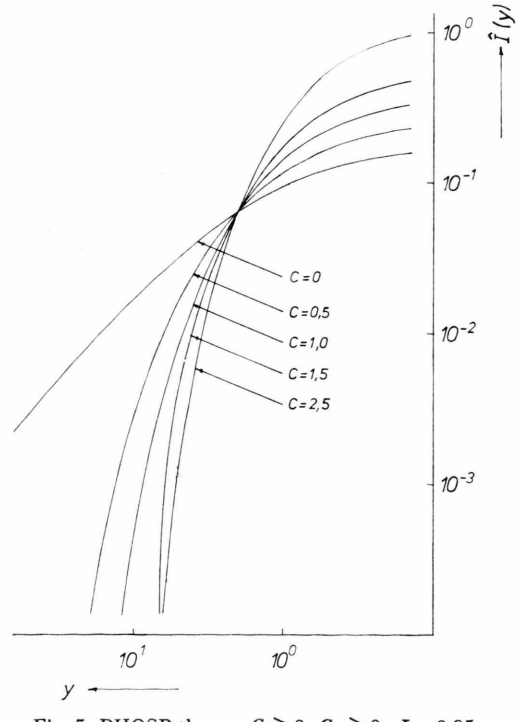

Fig. 5. PHQSB-theory, $C_6>0$, $C_{12}>0$; $L=0.95$; C-dependence of the blue wing.

$V^i(r)$, characterized by the quantity L and on the relative depth of the initial state potential, characterized by C *.

We discuss first the L-dependence, assuming C to be constant (Figs. 2, 3). If $L \leqq 1$ (Fig. 2), then the value of the Boltzmann-Factor at $y=-1$ is comparable to unity, and the infinity at $y=-1$ clearly comes out. If, on the other hand, $L>1$, then $I(y)$ decreases rapidly, due to the Boltzmann-Factor, already at $|y|<-1$, so that the infinity at $y=-1$ remains hidden. In this case $I(y)$ is very small in the range $y>0$ (blue wing, Figure 3).

Next we discuss the C-dependence, assuming L to be constant (Figures 4, 5). It should be noted, that for a given system (fixed ε^i) the C-dependence of $I(y)$ reflects the temperature dependence of $I(y)$. If $C=\varepsilon^i/kT$ is not too small and if $L>1$, the red wing (Fig. 4) displays an inflection point related to the Minimum of $V^i(r)$. With increasing C the absolute value of the slope of $I(y)$ at the inflection point decreases; for $C>3$ $I(y)$ passes through a relative maximum at $|y|<-1$. In the blue wing ($y>1$, Fig. 5) $I(y)$ decreases monotonically, the slope of $I(y)$ at a fixed y-value increases with C. All C-curves intersect at a certain value of $y=y_s$. This is because $V^i(r)=0$ for $r=r(y_s)$. For L.-J.-6-12-potentials one has $|y_s|=4\,(-L^{-6}+L^{-12})$.

2) $C_6>0$, $C_{12}<0$

In this case the sum in (10) reduces to a single term over the whole r-range. Using the abbreviations

$$f'=(1-y/2)/(1-y)^{1/2};\ f_1'=-1+(1-y)^{1/2},$$
$$\cdot V_1'(L,y)=-2\,L^6 f_1'(y)\ L^{12} f_1'^2(y) \qquad (15)$$

one obtains for $y<0$ (red wing)

$$I(y,L,C)=\frac{\sqrt{2}}{3}\,h\,n\,\frac{\sigma^3}{\varepsilon} \qquad (16)$$
$$\cdot y^{-2}\{|1+f'(y)|\,|f_1'(y)|^{1/2}\exp[-C\,V_1'(L,y)]\}.$$

In the range $y>0$ (blue wing) the intensity becomes zero. Contrary to case 1), there is no infinity at $y=-1$ in case 2), for in this case no extremum exists in $V(r)$. The L- and C-dependence of $I(y)$ (Figs. 6, 7) is, however, similar as in case 1).

* In Figs. 2–7 the reduced quantity $\hat{I}=I/\left(\frac{\sqrt{2}}{3}\,h\,n\,\frac{\sigma^3}{\varepsilon}\right)$ is plotted.

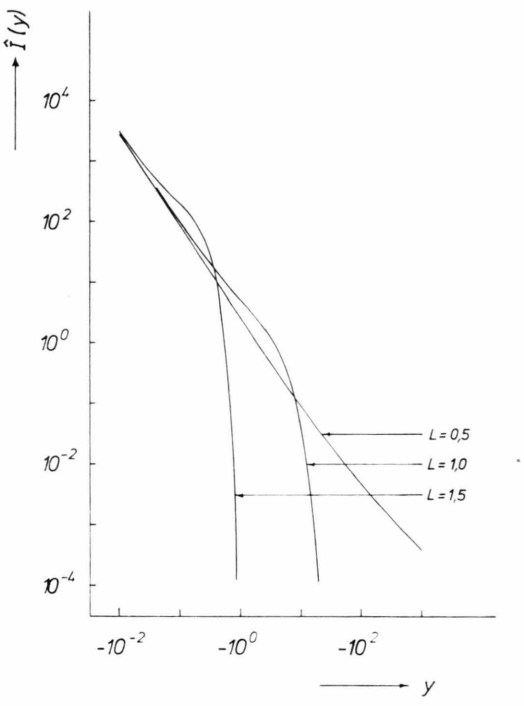

Fig. 6. PHQSB-theory, $C_6>0$, $C_{12}<0$; $C=1.0$; L-dependence of the red wing.

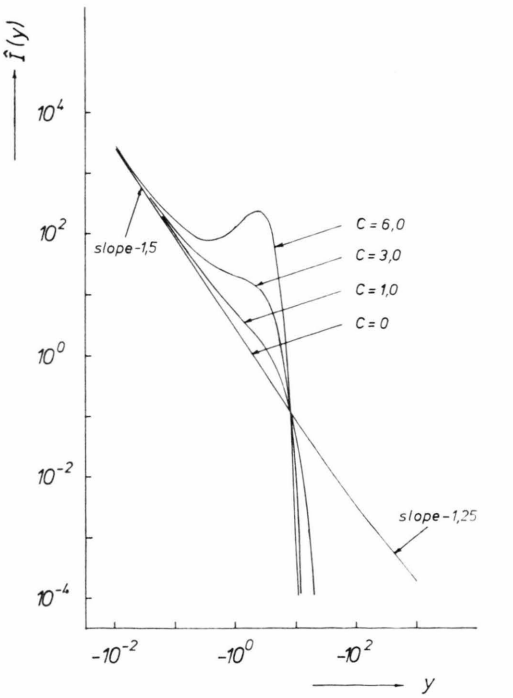

Fig. 7. PHQSB-theory, $C_6>0$, $C_{12}<0$; $L=1.0$; C-dependence of the red wing.

4. Criteria of Validity

It is well known that the quasistatic theory may be considered as a special case of the phase shift theory of collision broadening [11]. In subsection 4.1 the condition will be discussed, under which the intensity distribution resulting from the PHQSB-theory is identical to that obtained from the phase shift theory. It will be seen, that this is, in general, true only for certain spectral ranges of the wings. In 4.2 the validity condition of the phase shift theory, namely the condition for adiabatic collisions, which is at the same time a validity condition of the PHQSB-theory, will be discussed.

4.1 The PHQSB-theory as Special Case of the Phase Shift Theory

A general validity criterium for the PHQSB-theory as a special case of the phase shift theory may be derived by Fourier analysis of the phase disturbed dipole oscillation during the collision [12, 13]. Using the method of stationary phase, it may be shown, that the spectral intensity distribution may be interpreted as quasistatic only in certain frequency ranges, where the condition

$$R(t_k) = |\Delta\ddot{\omega}(t_k)|\,|2/\Delta\dot{\omega}(t_k)|^{3/2} \ll 1 \qquad (17)$$

is fulfilled. In (17) the time t_k is defined by

$$\Delta\omega(t_k) = \omega - \omega_0 \equiv \omega' \qquad (18)$$

where ω_0 is the unperturbed eigenfrequency of the oscillator and ω the frequency of the radiation emitted or absorbed. In order to determine the frequency ranges, where (17) is fulfilled, $R(t_k)$ has to be calculated. For this purpose we consider binary collisions and assume the straight path-constant velocity model for the collision (impact parameter ϱ, average velocity $\bar{v}$). For L.-J.-6-12-interaction one obtains [14]:

$$R(t_k) = S(c,x) = K\left(\frac{1}{\alpha}\right)^{1/2} \frac{1}{c^{5/12}} \frac{1}{|1-2c|^{1/2}} \left\{ 4\,\frac{-2+7c}{|1-2c|}\,(1-x^2)^{1/4} + (1-x^2)^{-3/4} \right\}$$

with

$$K = \frac{1}{3^{3/2}} \left| \frac{1}{2}\,\frac{c_6^{11/6}}{c_{12}^{5/6}} \right|^{1/2}; \quad c_6 = \frac{3\pi}{8}; \quad c_{12} = \frac{63\pi}{256};$$

$$\alpha = 2\,\frac{c_6^{11/6}}{c_{12}^{5/6}}\,\frac{\varepsilon\sigma}{\hbar\bar{v}}; \quad x = \frac{\varrho}{r(t_k)} = \frac{\varrho}{\sigma}\,c^{1/6}(\omega'); \quad 0<x<1; \qquad (19)$$

$$c(\omega') = \left(\frac{\sigma}{r(t_k)}\right)^6 = \begin{cases} \frac{1}{2}(1 \pm \sqrt{1+\hbar\omega'/\varepsilon}) & \text{if } C_6>0,\ C_{12}>0,\ \omega'<0 \\ \frac{1}{2}(1+\sqrt{1+\hbar\omega'/\varepsilon}) & \text{if } C_6>0,\ C_{12}>0,\ \omega'>0 \\ \frac{1}{2}(-1+\sqrt{1-\hbar\omega'/\varepsilon}) & \text{if } C_6>0,\ C_{12}<0,\ \omega'<0. \end{cases}$$

1) $C_6>0$, $C_{12}>0$

For $\omega'>0$ (blue wing) and $\hbar\omega'/\varepsilon \gg 1$ (19) simplifies and one obtains:

$$R(t_k) = 2^{5/12}\cdot K\cdot\left(\frac{1}{\alpha}\right)^{1/2}\left(\frac{\varepsilon}{\hbar\omega'}\right)^{\frac{11}{24}} f(x); \qquad (20)$$

with

$$f(x) = \{14(1-x^2)^{1/4} + (1-x^2)^{-3/4}\}.$$

From (20) there follows the existence of a frequency limit ω_L', so that for $\omega' \gg \omega_L'$ (17) is fulfilled. Denoting by x_L an arbitrary value for x, for which $1-x_L \ll 1$, and defining ω_L' by requiring $R(t_k)=1$, one obtains from (20)

$$\omega_L' = 2^{\frac{10}{11}}\,|K\cdot f(x_L)|^{\frac{24}{11}}\,(1/\alpha)^{\frac{12}{11}}\,\varepsilon/\hbar. \qquad (21)$$

To the frequency limit ω_L' there corresponds a critical impact parameter ϱ_L, given by

$$\varrho_L = x_L\,\sigma\,\frac{1}{c^{1/6}(\omega_L')} \qquad (22)$$

so that condition (17) is fulfilled for collisions with $\varrho \ll \varrho_L$.

If $\omega'<0$ (red wing), condition (17) is fulfilled in the range

$$0<\delta_1(\alpha)<|\hbar\omega'/\varepsilon|<\delta_2(\alpha)<1, \quad \text{if} \qquad (23)$$

$$\alpha \geqq \alpha_0(x_L). \qquad (24)$$

In (24) $\alpha_0(x_L)$ is defined by the requirement $S(c_{\min}, x_L) = 1$; here $c_{\min}$ is a value of c, for which $c^{-5/12}\cdot|1-2c|^{-1/2}$ becomes a minimum; x_L is a value of x, for which $1-x_L \ll 1$ and for which the second term in the brackets of (19) becomes large compared to the first term. The limits $\delta_1(\alpha)$, $\delta_2(\alpha)$ are the wider, the larger α is compared to α_0.

Alternatively, for systems with $C_6>0$, $C_{12}>0$ and $a \leqq a_0(x_L)$, i. e. for high temperatures, condition (17) is not fulfilled and consequently the PHQSB-theory invalid in the red wing.

2) $C_6>0$, $C_{12}<0$

In this case only for $\omega'<0$ the intensity will be unequal zero. (17) is fulfilled in the range $\omega' \gg \omega_L'$, where ω_L' is given by (21). Similarly a critical impact parameter ϱ_L exists, given by (22).

4.2 The Criterium of Adiabaticity

We restrict ourselves to cases, where collision induced transition between fine- and hyperfine structure states of the unperturbed atom (J-mixing collisions) may be neglected and only transitions between magnetic substates (m-mixing collisions) may occur with nonvanishing probability.

Denoting by $V^f_{m'}(t)$ and $V^f_m(t)$ the time dependent perturbations for the substates m and m′ and by τ_c the collision time, the condition for the collisions to be adiabatic is [15]

$$1/\tau_c \ll \left(\frac{V^f_{m'}(t) - V^f_m(t)}{\hbar} \right) . \qquad (25)$$

This condition may be written in a more rigorous manner [16]

$$\Delta\eta = (1/\hbar) \int \left(V^f_{m'}(t) - V^f_m(t) \right) dt \gg 1 . \qquad (26)$$

If in particular $V^f_{m'}(r(t))$ and $V^f_m(r(t))$ are approximated by L.-J.-functions and assuming the straight path-constant velocity model for the collisions, condition (26) becomes

$$\Delta\eta = \frac{1}{\hbar\, \bar{v}} \left| - \frac{c_6\, \Delta C_6}{\varrho^5} + \frac{c_{12}\, \Delta C_{12}}{\varrho^{11}} \right| \gg 1 \qquad (27)$$

where $\Delta C_6 = C^f_{6m'} - C^f_{6m}$ and $\Delta C_{12} = C^f_{12m'} - C^f_{12m}$. Thus a critical impact parameter ϱ_c [not to be confused with the impact parameter ϱ_L, defined by (22)], defined by $\Delta\eta(\varrho_c) = 1$, exists, so that collisions with $\varrho \ll \varrho_c$ are adiabatic. Together with the result of subsection (4.1) one may conclude, that the PHQSB-theory is applicable for collisions with

$$\varrho \ll \min(\varrho_c, \varrho_L) .$$

III. Experimental Details and Results

1. The Optical Arrangement

The measurements of the spectral distribution of the absorption coefficient in the neighborhood of the perturbed atomic line were performed using a conventional single beam arrangement: A beam of monochromatic light with a certain spectral bandwidth, selected out of the continuous spectrum of a background source using a monochromator, was passed through the absorption tube and its intensity measured photoelectrically. A commercial Deuterium lamp was used as the background source, the spectral selection was achieved by means of a Zeiss prism double monochromator. Using slit widths of about 0.1 mm, the band width of the light beam was about 1.5 Å at $\lambda = 2537$ Å. There, the inaccuracy of the wavelength setting was less then 0.25 Å. The light beam was chopped at a frequency of 450 cycles/sec, and the corresponding a. c. current from a 1P28-multiplier, after linear amplification and rectification, was registered using a multiflex galvanometer.

2. The Absorption Tube

The absorption tube was of conventional type, made of a quartz cell 30 cm long and 3 cm in diameter, with plane quartz windows at the ends. For the investigation of the Hg-Hg interaction a small amount of Hg was distilled into the highly evacuated cell, which was melt off thereafter. In order to study the Hg-Ar interaction, in addition spectrally pure Ar, at a number density of 1.26×10^{19} cm^{-3} was introduced. The maximum temperature of about 600 °K was produced by a commercial oven; temperature homogeneity along the tube length (maximum variation about 0.2 °K) was achieved by means of additional heating coils in front of the windows. Temperature fluctuations in the cell during the measurements were kept below 0.01 °K. Details of the construction of the whole heating arrangement and the regulation and measurement of the temperature have been described elsewhere [7].

3. The Measurement of the Absorption Coefficient

The spectral distribution of the absorption coefficient $k(\Delta\tilde{\nu})$ in the line wings was derived from measurements of the spectral distribution of the intensity transmitted by the absorption cell, once with mercury in it ($I(\Delta\tilde{\nu})$, at elevated temperature) and once without mercury ($I_0(\Delta\tilde{\nu})$, at room temperature). $k(\Delta\tilde{\nu})$ was then obtained from the well known relation $I(\Delta\tilde{\nu}) = I_0(\Delta\tilde{\nu}) \exp[-k(\Delta\tilde{\nu})l]$, where l is the tube length. This procedure required an extremely high stability of the whole arrangement. It was controlled by checking whether at large $\Delta\tilde{\nu}$, i. e. at vanishing absorption, the measured functions $I(\Delta\tilde{\nu})$ and $I_0(\Delta\tilde{\nu})$ merged into each other.

The wings of the absorption line were measured with 4 different densities of mercury vapor (n_{Hg} between 7.4×10^{16} and $3.36\times10^{18}\,cm^{-3}$, corresponding to temperatures between 427 and 563.5 °K), yielding sufficiently absorption in the wings.

From the measurements of the selfbroadening of the mercury line it was found, that its contribution to the absorption coefficient observed in the presence of Ar, is considerable at mercury densities of the order of $10^{18}\,cm^{-3}$, especially in the red wing. The absorption coefficient $k_{Hg-Ar}(\Delta\tilde{\nu},T)$ due to the Hg – Ar interaction alone was obtained from

$$k_{Hg-Ar}(\Delta\tilde{\nu},T)=k_{tot}(\Delta\tilde{\nu},T)-k_{Hg-Hg}(\Delta\tilde{\nu},T) \tag{28}$$

where $k_{Hg-Hg}(\Delta\tilde{\nu},T)$ and $k_{tot}(\Delta\tilde{\nu},T)$ are the absorption coefficients obtained from measurements with pure Hg in the cell and with a Hg – Ar mixture, respectively.

The relation (28) certainly holds under the assumptions of the binary approximation of the quasistatic theory.

4. Results

In order to obtain a single profile, the reduced absorption coefficient $k(\Delta\tilde{\nu})/Nn$ (N, n, number densities of the active atom and perturbing atom respectively) was plotted. Because of the large ranges involved a double logarithmic scale was used. Figures 8 – 11 show the final plots.

1) System Hg 2537/Ar

Our study is an extension of Kuhn's [17] photographic measurements of the near wings (up to $|\Delta\tilde{\nu}|\approx 250\,cm^{-1}$) to larger frequency distances from the unperturbed line. We find the red wing, between -100 and $-250\,cm^{-1}$ following very closely a $\Delta\tilde{\nu}^{-3/2}$-law, in agreement with Kuhn's observation. Also, our absolute values of $k(\Delta\tilde{\nu})/Nn$ in this region agree with those of Kuhn, within 10%. In the region beyond $250\,cm^{-1}$, not investigated by Kuhn, the slope of $k(\Delta\tilde{\nu})$ is seen to increase monotonically with $\Delta\tilde{\nu}$. In the blue wing two satellites with peaks at $\Delta\tilde{\nu}=71.5\,cm^{-1}$ and $168\,cm^{-1}$ appear, as reported by Kuhn. In the range beyond the outer satellite $k(\Delta\tilde{\nu})$ decreases monotonically.

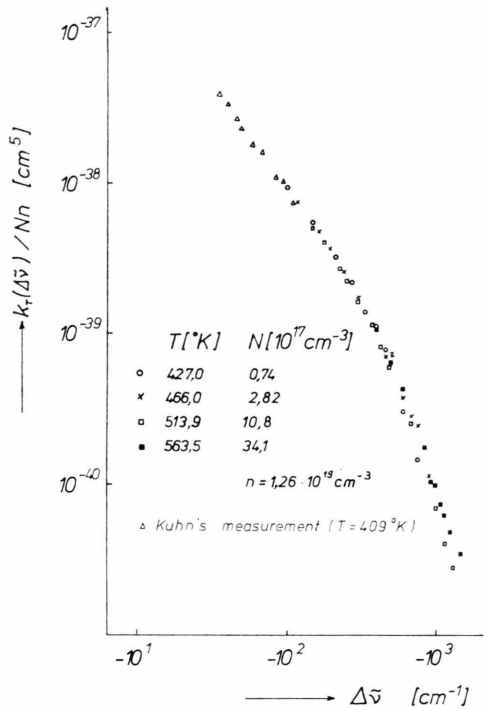

Fig. 8. Red wing of the Hg-absorption line λ 2537 Å, perturbed by Ar.

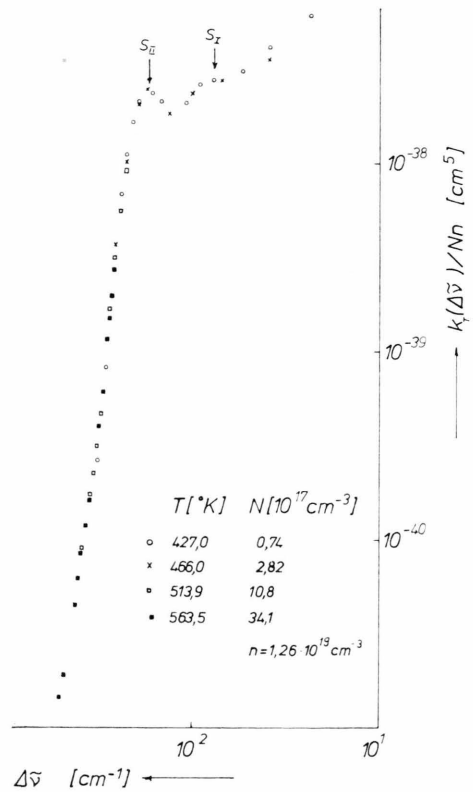

Fig. 9. Blue wing of the Hg-absorption line λ 2537 Å, perturbed by Ar.

2) System Hg 2537/Hg

The near wings, as in the case of Hg 2537/Ar, have been studied by Kuhn [17], the red wing up to $\Delta\tilde{\nu} = -1000\,\mathrm{cm}^{-1}$ and the blue wing up to $\Delta\tilde{\nu} = 30\,\mathrm{cm}^{-1}$. Like with Hg 2537/Ar, our measurements are extensions of those of Kuhn to larger distances from the unperturbed line. Our results agree well with those of Kuhn.

IV. Qualitative Interpretation of the Results

Apart from the two blue satellites in the case Hg 2537/Ar, which are probably of molecular origin [18], the observed features of $k(\Delta\tilde{\nu})$ are in qualitative agreement with the theoretical predictions. The absence of any other satellites in the spectral range investigated indicates, that extrema in the difference potentials are either not existing ($C_6>0$, $C_{12}<0$; $C_6<0$, $C_{12}>0$) or are hidden due to the effect of the Boltzmann-Factor ($C_6>0$, $C_{12}>0$, $L>1$; $C_6<0$, $C_{12}<0$, $L>1$). In any case the large absolute values of the slopes of $k(\Delta\tilde{\nu})$ at sufficiently large $|\Delta\tilde{\nu}|$ are most probably due to the combined effect of the Boltzmann-Factor and the large values of $|\mathrm{d}V(r)/\mathrm{d}r|$. The inflection point of $k(\Delta\tilde{\nu})$ in the red wing of Hg 2537/Hg may be attributed to the minimum of $V^{\mathrm{i}}(r)$.

For a more quantitative interpretation it is necessary to consider the splitting of the $^3P_1$ state of the Hg atom into substates with space quantum numbers $m_J = 0$ and ± 1. To these substates there correspond two distinct molecular states of the diatomic system, composed of a mercury atom in its $^3P_1$ state and an argon atom in its $^1S_0$ ground state, and which are labelled in the notation of Herzberg [19], $B\,^3\Sigma_1$ and $A^3\Pi_0$ respectively *. The system with both atoms in the ground state is labelled $X\,^1\Sigma_0$.

We denote the respective adiabatic potential functions by $V_\Sigma^{\mathrm{f}}(r)$, $V_\Pi^{\mathrm{f}}(r)$ and $V^{\mathrm{i}}(r)$, the corresponding difference potentials by $V_\Sigma(r) = V_\Sigma^{\mathrm{f}}(r) - V^{\mathrm{i}}(r)$ and $V_\Pi(r) = V_\Pi^{\mathrm{f}}(r) - V^{\mathrm{i}}(r)$.

Now, the determination of the potentials from the measurements is greatly simplified, if, for a given system, each wing is exclusively formed by transitions $X\,^1\Sigma_0 \rightarrow A^3\Pi_0$ *or* $X\,^1\Sigma_0 \rightarrow B\,^3\Sigma_1$. To decide this question, at least a rough knowledge of the relative magnitudes of the attractive and repulsive parts of the functions $V_\Pi(r)$ and $V_\Sigma(r)$ is necessary. For the system Hg 2537/Ar it may be expected from theoretical Van der Waals constants and the electron distributions for the Π- and Σ-states of the diatomic system, that $V_\Pi(r)<0$ and $V_\Sigma(r)>0$ over the whole r-range under investigation [6]. It then follows, that in this case the red wing should exclusively be formed by transitions $X\,^1\Sigma_0 \rightarrow A^3\Pi_0$ and the blue wing exclusively by transitions $X\,^1\Sigma_0 \rightarrow B\,^3\Sigma_1$. A similar reasoning may be applied to the system Hg 2537/Hg with the result, that also in this case $V_\Pi(r)<0$ and $V_\Sigma(r)>0$, so that the wings should be formed by the same transitions as in the case Hg 2537/Ar. Approximating the potential functions $V_\Pi(r)$ and $V_\Sigma(r)$ by those of the L.-J.-6-12-type, we assume then the following signs for the C_6's and C_{12}'s:

	$C_{6\Pi}$	$C_{6\Sigma}$	$C_{12\Pi}$	$C_{12\Sigma}$
Hg 2537/Ar	>0	<0	<0	>0
Hg 2537/Hg	>0	<0	<0	>0

By comparison with experiment it will turn out later, that these assumptions are not always strictly fulfilled. It will be seen, however, that the deviations do not affect the interpretation of the wings in the frequency range investigated.

V. The Determination of the L.-J.-parameters

In principle, the L.-J.-parameters C_6 and C_{12} are obtained by optimum adjustment of the theoretical to the experimental profiles. For this purpose comparison was made of calculated profiles, varying systematically C_6 and C_{12}, with the measured profile, until optimum agreement is obtained. This procedure has to be performed for each wing separately, since we assume, that, for a given system, the red wing and the blue wing are related to different potential functions.

For the calculation of $k(\Delta\tilde{\nu})$ we start from the intensity formulas (13) and (14) if $C_6>0$, $C_{12}>0$ (or $C_6<0$, $C_{12}<0$) and from formula (16) if $C_6>0$, $C_{12}<0$ (or $C_6<0$, $C_{12}>0$). The reduced quantity y is replaced by $\Delta\tilde{\nu} = \varepsilon y/hc$. To account for the influence of molecular formation, these formulas have to be multiplied by the function $g(r)$ given by (5), where r is related to $\Delta\tilde{\nu}$ by $hc\,\Delta\tilde{\nu} = V(r)$. For the L.-J.-parameters of the potentials

* In Ref. [6] the excited atomic states have erroneously been correlated to the molecular states $B^1\Sigma_0$ and $A^3\Pi_1$.

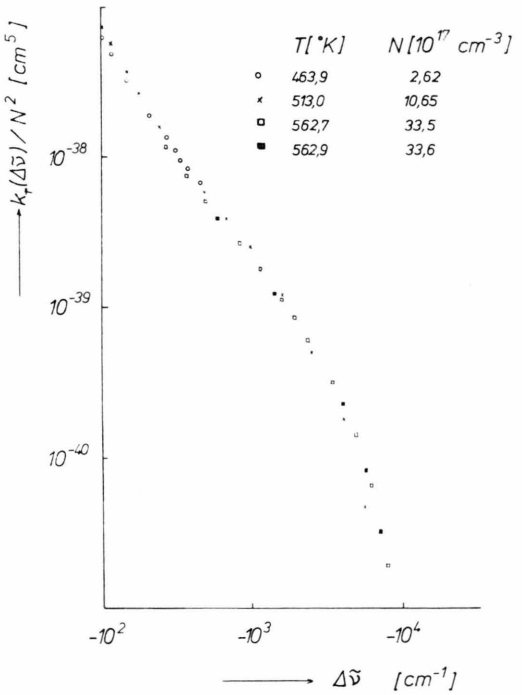

Fig. 10. Red wing of the selfbroadened Hg-absorption line λ 2537 Å.

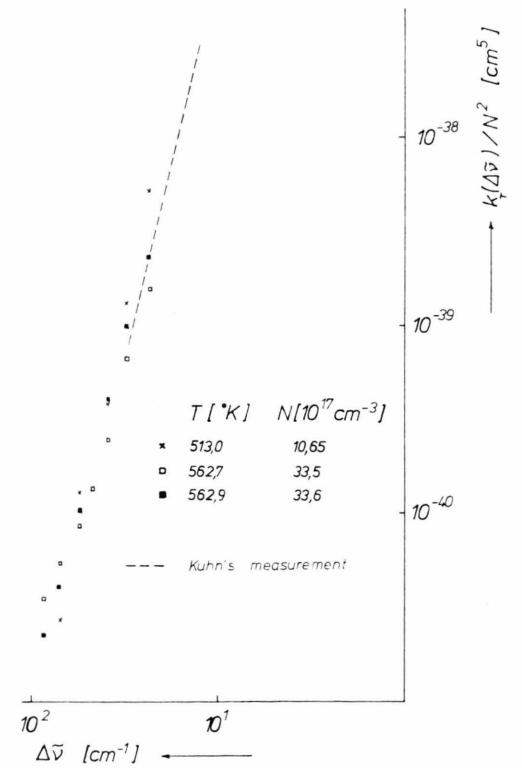

Fig. 11. Blue wing of the selfbroadened Hg-absorption line λ 2537 Å.

$V^i(r)$ of the initial state, entering the Boltzmann-Factor and $g(r)$, the following values were used: For $C_6{}^i$ the semi-empirical value reported by Heller [20] was taken; for $C_{12}{}^i$ the value determined from $C_6{}^i$ and the potential depth ε^i was taken, obtained from spectroscopic data (dissociation energy and zero point energy) reported by Oldenberg [21]. From the intensity $I(\Delta\tilde{\nu})$ the absorption coefficient $k(\Delta\tilde{\nu})$ is obtained from

$$k(\Delta\tilde{\nu}) = N^* f (\pi e^2/m c) I(\Delta\tilde{\nu}). \qquad (29)$$

(N^* effective number density of mercury atoms, f oscillator strength of the line = 0.0255, e, m charge and mass of the electron, c light velocity). The effective number density N^* of the mercury atoms involved in the tranistion $X\,^1\Sigma_0 \rightarrow A\,^3\Pi_0$ is $^2/_3 N$ and that involved in transitions $X\,^1\Sigma_0 \rightarrow B\,^3\Sigma_1$ is $\frac{1}{3} N$, N being the total number density of mercury atoms.

In the optimization procedure [7] for the determination of the L.-J.-parameters use of the fact was made, that, in the present cases, $k(\Delta\tilde{\nu})$ is at small $\Delta\tilde{\nu}$ mainly determined by the r^{-6} term and at large $\Delta\tilde{\nu}$ mainly by the r^{-12} term of the difference potential. The magnitude in the change of $k(\Delta\tilde{\nu})$ by changing C_{12} is illustrated for the red wing of the system Hg 2537/Ar in Figure 12.

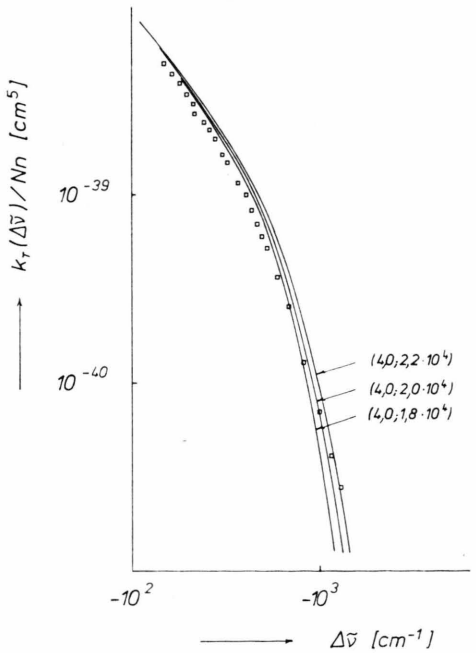

Fig. 12. Red wing of the Hg-absorption line λ 2537 Å, perturbed by Ar; on the determination of $C_{12\Pi}$. □ □ □ measurement at 513 °K; ——— theoretical curves (C_6 eVÅ^6; $-C_{12}$ eVÅ^{12}); Π optimum adjustement obtained for $C_{6\Pi} = (4 \pm 1)$ eVÅ^6, $C_{12\Pi} = -(2 \pm 0.2) \times 10^4$ eVÅ^{12}.

The evaluation of $C_{6\Sigma}$ and $C_{12\Sigma}$ from the blue wing in the case Hg 2537/Ar by means of the procedure described above causes difficulties, since there the continuum due to unbound pairs is superimposed by satellites. These satellites are possibly related to Hg – Ar-molecules, since their intensity decreases with temperature[18]. For this reason Michels et al.[18] have interpreted the continuum on the short wavelength side of the outer satellite (S_{II}, Fig. 9) by transitions between discrete molecular ground-states and continuous upper states. According to quantum calculations reported by these authors $k(\Delta\tilde{\nu})$ is expected to be

$$\ln k(\Delta\tilde{\nu}) \sim (\ln(\Delta\tilde{\nu}/\Delta\tilde{\nu}_{max}))^2 \qquad (30)$$

where $\Delta\tilde{\nu}_{max} = 170\ cm^{-1}$ is the position of the maximum of S_{II}. The authors find agreement between their calculations and the measurements up to $260\ cm^{-1}$ reported by Kuhn[17]. Measurements in the present investigation performed up to about $500\ cm^{-1}$, however, deviate beyond about $290\ cm^{-1}$ from the theoretical curve (Figure 13). In this region the measured absorption is larger than the calculated one. The additional absorption shall tentatively be interpreted by transitions between unbound states (free-free transitions), on the basis of the PHQSB-theory. According to this theory the absorption observed above $\Delta\tilde{\nu}(r=\sigma^i)$ should be exclusively caused by free-free-transitions, if $C_{12}>0$. These free-free transitions are not accounted for by Michels et al. For the determination of $C_{6\Sigma}$ and $C_{12\Sigma}$ the theoretical $k(\Delta\tilde{\nu})$-curve, accounting only for free-free transitions, was fitted to that measured above $400\ cm^{-1}$ (Fig. 14) assuming, that in this region the contribution $k_T{}^b(\Delta\tilde{\nu})$ of bound-free tran-

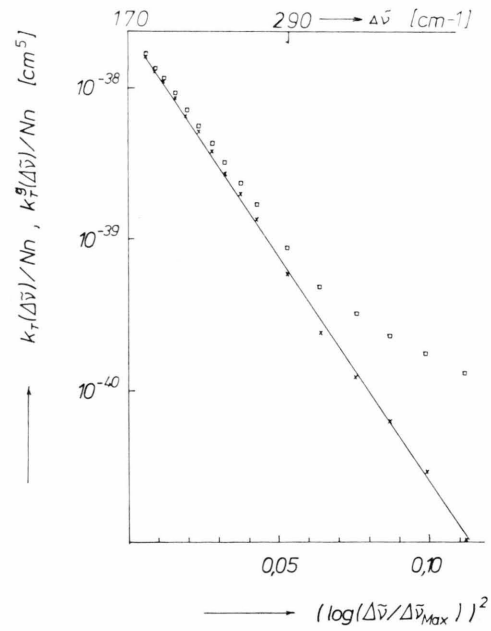

Fig. 13. Blue wing of the outer satellite S_{II} of the Hg-absorption line λ 2537 Å, perturbed by Ar; □□□ measurement at 513.9 °K; ××× absorption coefficient $k_T{}^b(\Delta\tilde{\nu})/nN$ for bound-free transitions.

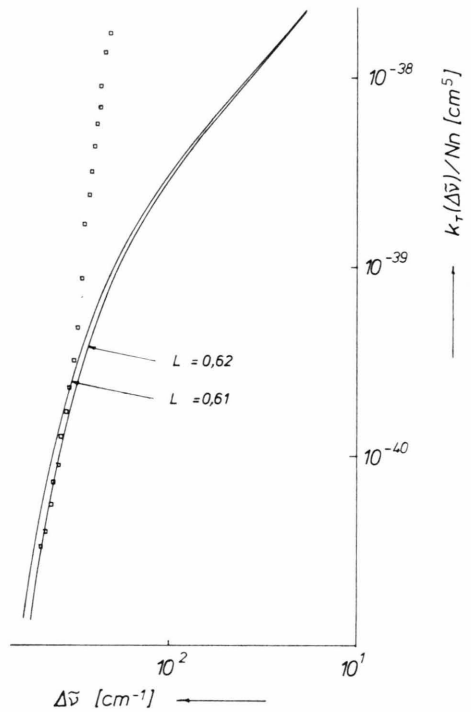

Fig. 14. Blue wing of the Hg-absorption line λ 2537 Å, perturbed by Ar. □□□ measurement at 513.9 °K; ——— theoretical curves $k_T{}^f(\Delta\tilde{\nu})$ for $C_{6\Sigma}=0.83$ eVÅ^6.

Table 1. Lennard-Jones parameters for the systems Hg 2537/Ar and Hg 2537/Hg.

	C_6 (eVÅ^6)	C_{12} (10^4 eVÅ^{12})	ε (eV)	r_m (Å)
Hg 2537/Ar				
VII (red wing)	4 ±1	−2.0 ±0.2		
V_Σ (blue wing)	0.8	0.93±0.01	1.7×10^{-5}	5.33
Vi	66.1	4.1	2.7×10^{-2}	3.28
VII^f	70.1	2.1	5.8×10^{-2}	2.90
$V_\Sigma{}^f$	66.9	5.0	2.2×10^{-2}	3.39
Hg 2537/Hg				
VII (red wing)	270 ±50	−4 ±1		
V_Σ (blue wing)	2.5± 0.5	0.14±0.02	1.1×10^{-3}	3.22
Vi	143	5.97	8.5×10^{-2}	3.05
VII^f	413	2.0	2.1	2.14
$V_\Sigma{}^f$	146	6.1	8.8×10^{-2}	3.06

sitions is negligable. When the measured absorption coefficient $k_T^{exp}(\Delta\tilde{\nu})$ is corrected for the contribution $k_T^f(\Delta\tilde{\nu})$ due to free-free transitions, the resulting absorption $k_T^b(\Delta\tilde{\nu}) = k_T^{exp}(\Delta\tilde{\nu}) - k_T^f(\Delta\tilde{\nu})$ is well accounted for by (30) over the whole $\Delta\tilde{\nu}$-range (up to 500 cm^{-1}) investigated.

The L.-J.-parameters of the difference potentials $V(r)$ for both systems, determined by means of the procedures described above, are collected in Table 1. The parameters of the potentials $V^i(r)$ and $V^f(r) = V(r) + V^i(r)$ are also included. The potential curves are plotted in Figures 15, 16.

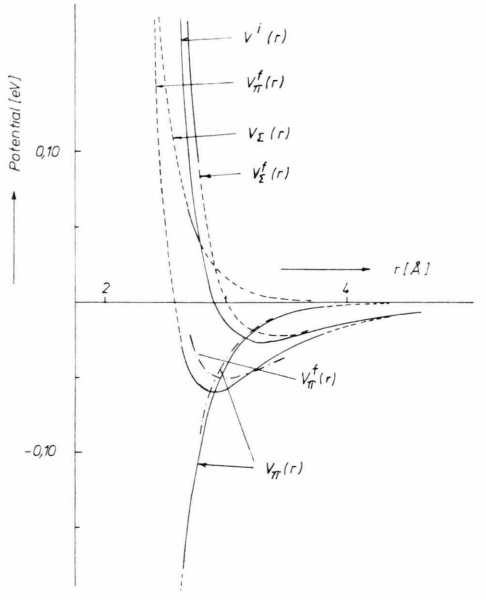

Fig. 15. L.-J.-potential curves of the system Hg 2537/Ar; ——— curve parts obtained from measurement (indirect method); – – – curve parts not obtained from measurement (indirect method); –·–·– curve parts obtained from measurement (direct method)[6].

The parameter C assumes the following values in our experiment:

Hg 2537/Ar		Hg 2537/Hg	
T (°K)	C	T (°K)	C
427	0.72	463.9	2.14
466	0.66	513.0	1.93
513.9	0.60	562.7	1.76
563.5	0.55	562.9	1.76

The parameter L assumes the following values:

Hg 2537/Ar $L_\Pi = 0.70$; $L_\Sigma = 0.61$;
Hg 2537/Hg $= 1.19$; $= 0.95$.

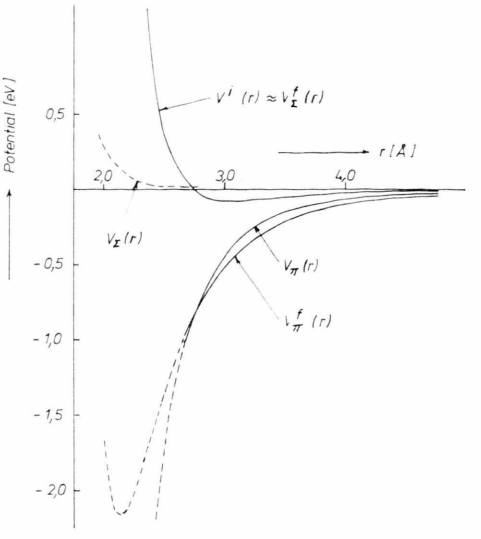

Fig. 16. L.-J.-potential curves of the system Hg 2537/Hg; ——— curve parts obtained from measurement (indirect method); – – – curve parts not obtained from measurement (indirect method).

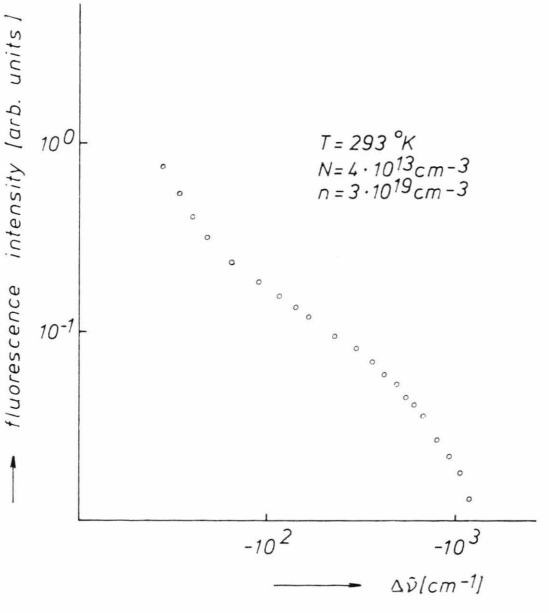

Fig. 17. Red wing of the Hg-emission line λ 2537 Å, perturbed by Ar.

VI. Discussion

1. The Potential Functions

The potential curves of the systems Hg 2537/Ar and Hg 2537/Hg in comparable states show similar features (Figs. 15, 16); they shall be discussed,

therefore, together. We denote by r_m^i, $r_{m\Pi}^f$, $r_{m\Sigma}^f$ and ε^i, ε_Π^f, ε_Σ^f the position and the depths of the minima of the potential functions $V^i(r)$, $V_\Pi^f(r)$, $V_\Sigma^f(r)$, respectively.

Regarding $V_\Pi(r)$, it is seen from Table 1, that $C_{6\Pi}>0$ and $C_{12\Pi}<0$. This is in agreement with the assumption (s. Chapter IV). Figures 15, 16 show, that $r_{m\Pi}^f<r_m^i$ and $\varepsilon_\Pi^f>\varepsilon^i$.

In $V_\Sigma(r)$ both $C_{6\Sigma}$ and $C_{12\Sigma}$ are found to be positive (Table 1). $C_{12\Sigma}>0$ is in disagreement to the assumption (s. Chapter IV). The depths ε_Σ of $V_\Sigma(r)$, however, amount to be 1.7×10^{-5} eV in case of Hg 2537/Ar and $\approx1.1\times10^{-3}$ eV in case of Hg 2537/Hg. To these values of ε_Σ there correspond cutoffs in the binary quasistatic intensity distribution at $-0.14\,\mathrm{cm}^{-1}$ and $\Delta\tilde{\nu}=-9\,\mathrm{cm}^{-1}$. Thus, the contribution of $V_\Sigma(r)$ to the formation of the red wings beyond $100\,\mathrm{cm}^{-1}$, measured in this investigation, will be negligable. Figures 15, 16 show, that $r_{m\Sigma}^f>r_m^i$ and $\varepsilon_\Sigma^f<\varepsilon^i$.

It should be noted, that, with respect to the relative depth and position of the minima, the experimental potential curves $V^i(r)$, $V_\Pi^f(r)$ and $V_\Sigma^f(r)$ for the states $X\,^1\Sigma_0$, $A\,^3\Pi_0$ and $B\,^3\Sigma_1$ of the systems considered agree qualitatively with theoretical curves for the states $X\,^2\Sigma$, $A\,^2\Pi$ and $B\,^2\Sigma$ of the systems alkali-noble gas [22]. This may be explained by means of theoretical values for the C_6's and electron distributions in the Π- and Σ-states of the systems [6].

For the values $C_{6\Pi}$ and $C_{12\Pi}$ of the system Hg 2537/Ar, obtained from optimum adjustment, the agreement of experimental and theoretical $k(\Delta\tilde{\nu})$-curves is only moderate (Figure 12). This means, that the L.-J.-function is, in this case, only a rough approximation to the true potential function.

2. *The Assumptions of the Theory*

In order to test the reliability of the potential parameters let us first examine whether the validity conditions (17) or (21) and (27) of the PHQSB-theory are fulfilled. From Table 2 it may be seen, that the frequency ranges investigated ($|\Delta\tilde{\nu}|>200\,\mathrm{cm}^{-1}$) are well beyond the frequency limits $\Delta\tilde{\nu}_L$. On the other hand, the values of $R(t_k)$ at $|\Delta\tilde{\nu}_L|=200\,\mathrm{cm}^{-1}$ (Table 3) are not very small compared to unity. This means, that in the neighborhood of $\pm200\,\mathrm{cm}^{-1}$, the lower limit of the range investigated, the condition $R(t_k)\ll1$ is only moderately fulfilled. With increasing $|\Delta\tilde{\nu}|$, however, this condition will be fulfilled increasingly better.

Table 2. Values of $\Delta\eta(\varrho=\varrho_L)$ and $\Delta\tilde{\nu}_L$ with $x_L=0.98$.

System	Red wing $\Delta\eta_L$	Red wing $\Delta\tilde{\nu}_L$ [cm^{-1}]	Blue wing $\Delta\eta_L$	Blue wing $\Delta\tilde{\nu}_L$ [cm^{-1}]
Hg 2537/Ar	7.3	−50	1.7×10^1	54
Hg 2537/Hg	9.6	−20	1.5×10^3	37

Table 3. Values for $R(t_k)$ at $|\Delta\tilde{\nu}|=200\,\mathrm{cm}^{-1}$ with $x_L=0.98$.

System	Red wing	Blue wing
Hg 2537/Ar	0.54	0.56
Hg 2537/Hg	0.42	0.47

The adiabaticity criterium $\Delta\eta\gg1$ is fulfilled very well in the range $|\Delta\tilde{\nu}|>|\Delta\tilde{\nu}_L|$ (Table 2) in all cases.

The assumption of binary collisions (equivalent to assumption b) in II,1) has been discussed elsewhere [6]. A rough estimate shows, that it is well fulfilled for both systems investigated at the small particle number densities used.

Whether the oscillator strength f of the Hg line is constant over the range of internuclear distances r involved (assumption c) in II,1) must be regarded as uncertain. There is some experimental indication [23], however, that for the system Hg 2537/Ar f is constant for r-values larger than 2.45 Å.

The question whether resonance interaction in case of Hg 2537/Hg is of importance in the formation of the wings has been treated by Kuhn [5]. Because of the large range of the resonance forces ($V(r)\sim-r^{-3}$), at large Hg-number densities as used in this investigation, the resonance interaction will be highly multiple. Thus the interactions of several neighboring atoms mainly cancel each other, and its effect on the wings is excepted to be completely negligable. Actually a $\Delta\tilde{\nu}^{-3/2}$-law is being observed in the red wing of Hg 2537/Hg in the range between -10 and $-100\,\mathrm{cm}^{-1}$ [17] indicating pure Van der Waals interaction ($V(r)\sim-r^{-6}$) to be effective.

3. *Comparison with Potentials from other Experimental data*

It is of importance to compare the potential functions obtained from the far wings with those derived

from other experimental data. These are halfwidth and shift, satellite bands, temperature dependence of the wings and the profiles of the emission line.

3.1 Halfwidth and Shift

At most two potential parameters may be derived from halfwidth and shift, whereas the potential functions $V_{\Sigma}(r)$ and $V_{\Pi}(r)$ contain four parameters. In the case Hg 2537/Ar Schuller et al.[24] have determined these by the additional use of the experimental crossections for collisional depolarization of the resonance radiation and the theoretical value for $C^{f}_{6\Pi}/C^{f}_{6\Sigma}$. Since these authors assumed $C_{12\Pi}>0$, unfortunately their results cannot be compared as yet with those obtained from line wing data.

In the case of Hg 2537/Hg the line core is mainly determined by resonance interaction: Lennuier et al.[25] found, within the experimental error limits, agreement between the measured halfwidth and that calculated assuming $V(r)\sim r^{-3}$. Therefore, unless the accuracy of the experimental method is not improved, no information on the L.-J.-parameters can be derived in this case from line core measurements.

3.2 Satellite Bands

In the case Hg 2537/Ar red bands in the range between -80 and $-210\,\mathrm{cm}^{-1}$ are observed both in emission and absorption[21], at sufficiently high resolution, and may be explained as due to HgAr molecules. In absorption their intensity is so small, that they do not interfere with the intensity measurement of the continuous absorption. The observed degradation of these bands toward short wavelengths indicates, that $r_{m}^{f}<r_{m}^{i}$. This would be in agreement with the qualitative behaviour of the function $V_{\Pi}^{f}(r)$ obtained from the continuous absorption in the far wing (Figure 15). For a more quantitative comparison, an analysis of the bands in terms of the potential curve $V_{\Pi}^{f}(r)$ would be highly desirible.

On the other hand, the blue satellites may be understood, if at least for one of the potential functions $V_{\Pi}^{f}(r)$, $V_{\Sigma}^{f}(r)$ the position of the minimum is, with respect to that of $V^{i}(r)$, shifted to larger r values. This is actually the case for $V_{\Sigma}^{f}(r)$, as obtained from the continuum beyond the outer blue satellite (Figure 15). This interpretation is qualitatively similar to that given by Michels et al.[18], who, however, did not take into account the splitting of $V^{f}(r)$.

In the case Hg 2537/Hg red bands between ≈ -40 and $-80\,\mathrm{cm}^{-1}$ are observed in absorption and to be ascribed to transitions between quantized states of the Hg_2 molecule[17]. An interpretation, however, by means of the potentials $V_{\Pi}^{f}(r)$ or $V_{\Sigma}^{f}(r)$, derived from the far wing continua, causes difficulties. Transitions $V^{i}(r)\rightarrow V_{\Pi}^{f}(r)$ should cause bands at much larger wavelengths, at least $-1000\,\mathrm{cm}^{-1}$ from the atomic line. On the other hand, transitions $V^{i}(r)\rightarrow V_{\Sigma}^{f}(r)$ should cause bands at distances less than $-9\,\mathrm{cm}^{-1}$ from the line, corresponding to $\varepsilon_{\Sigma}=1.1\times10^{-3}$ eV. It must be remembered, however, that the validity condition of the PHQSB-theory is poorly fulfilled in the range below $100\,\mathrm{cm}^{-1}$- so that the potential $V_{\Sigma}^{f}(r)$ derived from the continuum in this range could be largely in error.

3.3 The Temperature Dependence of $k(\Delta\tilde{\nu})$

A rigorous test of the interpretation of the present results would be to examine, whether the intensity distribution in the far wings can be discribed by the same potentials $V^{i}(r)$, $V_{\Pi}(r)$ and $V_{\Sigma}(r)$ at largely differing temperatures. In the far wings of both systems investigated, the absolute values of the slopes of $k(\Delta\tilde{\nu})$ are, due to the Boltzmann-Factor in the distribution function, expected to decrease with increasing temperature. The small variation of the temperature used in the present experiments, however, did not allow so far to varify this prediction.

3.4 The Profile of the Emission Line

Finally, the interpretation of the wings of the absorption line may be tested by measurements of the profiles of the fluorescence emission line. Whereas, for the systems discussed, the far wings of the absorption line will be largely determined, through the Boltzmann-Factor in the distribution function, by the potential $V^{i}(r)$, those of the emission line are governed by the potentials $V_{\Pi}^{f}(r)$ (red wing) and $V_{\Sigma}^{f}(r)$ (blue wing). Consider for example the case Hg 2537/Ar. Because there $\sigma_{\Pi}^{f}<\sigma^{i}$ (Fig. 14), the steep intensity decrease in the far red wing is expected to occur at $\Delta\tilde{\nu}$ values considerably larger than in the absorption case. Similarly, because $\sigma_{\Sigma}^{f}>\sigma^{i}$ (Fig. 15), in the far blue wing the intensity decrease should occur already at $\Delta\tilde{\nu}$-values smaller

than in the absorption case. Figure 17 shows preliminary results of measurements of the red wing of the fluorescence emission line Hg 2537/Ar. Comparison with the red wing of the absorption line (Fig. 8) shows indeed qualitative agreement with the prediction. A more detailed comparison with theory, however, has to be postponed until more experimental data are available.

[1] W. R. Hindmarsh, A. D. Petford, and G. Smith, Proc. Roy. Soc. (London) **297**, A 296 [1967].
[2] W. Behmenburg. J.Q.S.R.T. **4**, 177 [1964].
[3] J. M. Vaughan and G. Smith, Phys. Rev. **166**, 17 [1968].
[4] F. Rostas and J. L. Lamaire, J. Phys. B **4**, 555 [1971].
[5] H. Kuhn, Phil. Mag. **18**, 987 [1934].
[6] W. Behmenburg, Z. Naturforsch. **27 a**, 31 [1972].
[7] J. Losen, Diplomarbeit Saarbrücken 1972, unpublished.
[8] M. R. Granier, Ann. de Physique **4**, 383 [1969].
[9] W. R. Hindmarsh and J. M. Farr, "Collision Broadening of Spectral Lines by Neutral Atoms" in Proc. Quant. Electr. **2**, 143 [1972].
[10] D. G. McCartan and W. R. Hindmarsh, J. Phys. B **2**, 1396 [1969].
[11] E. Lindholm, Ark. Mat. Astr. Fys. **32**, A1 [1945].
[12] T. Holstein, Phys. Rev. **79**, 744 [1950].
[13] I. I. Sobelman, Fortschr. Phys. **5**, 175 [1957].
[14] W. Behmenburg, to be published.
[15] L. Spitzer, Phys. Rev. **58**, 348 [1940].
[16] F. Schuller and B. Oksengorn, J. de Physique **30**, 531 [1969].
[17] H. Kuhn, Proc. Roy. Soc. (London) **158**, A212 [1937]; **158**, A230 [1937].
[18] A. Michels, H. De Kluiver, and C. A. Ten Seldam, Physica **25**, 1321 [1959].
[19] G. Herzberg, Molecular Spectra and Molecular Structure, D. Van Nostrand Co., New York 1950, Vol. 1.
[20] R. Heller, J. Chem. Phys. **9**, 154 [1941].
[21] O. Oldenberg, Z. Phys. **47**, 184 [1928]; **55**, 1 [1929].
[22] W. E. Baylis, J. Chem. Phys. **51**, 2665 [1969].
[23] J. C. Strijland and A. J. Nanassy, Physica **24**, 985 [1958].
[24] J. Butaux, F. Schuller, and R. Lennuier, J. de Physique **33**, 635 [1972].
[25] M. R. Lennuier and D. Perrin-Lagarde, C. R. Acad. Sci. Paris **247 B**, 1020 [1972].